

## Механика на непрекъснатите среди

### Numerical investigation of wave propagation in layered media. Part 1. Propagation of SH-waves

G. Brankov, Ts. Ivanov, T. Angelov

#### 1. Introduction

In consequence of an impulse excitation in the earth's crust, like earthquake, explosion, etc., in all directions from the epicenter waves begin to propagate. Reaching interfaces and other inhomogeneities these waves refract, reflect and convert from one type into another. Thus the problem for determination of the displacement and stress fields, due to the complicated wave processes arises. In such general treatment, however, the problem is not solved yet. There are known analytical solutions for the cases of homogeneous, elastic, isotropic half-space, in which the wave processes are caused of excitations applied at the surface of the half-space [1]. Obtaining of numerical results from this analytical solutions faces computational difficulties. Different methods are proposed to solve numerically the problem. In most of them a half-space consisting of parallel layers is considered [1, 2, 3, 4]. Basing on the method described in [5, 6], a half-space with dipping layers is considered in [7, 8, 9, 10, 11].

In the present paper we investigate numerically the propagation of SH-waves in an elastic, isotropic half-space, consisting of dipping layers, solving appropriate initial, boundary-value problems. Finite element method (FEM) for spatial discretization and Wilson's  $\theta$ -method or discrete Fourier transform for time discretization are used. We are faced, however, to a principal difficulty — the half-space could not be discretized with finite elements. This imposes an artificial restriction in a finite domain, which requires setting of physically suitable boundary conditions on the additional boundary, because these boundaries must not reflect the waves back into the domain.

Similar subjects about the applying of boundary element method, constructing of "infinite" elements and "transmitting boundaries" are discussed in [2, 3, 4, 12, 13, 14, 15]. In contrast with these approaches here we impose classical boundary conditions — prescribed displacements and tractions, as well as boundary conditions of contact type — elastic or viscous.

#### 2. Statement of the problem

We consider the half-space  $|x| \leq \infty, |z| \leq \infty, y \leq 0$ , with three dipping layers constituting angles  $\alpha$  and  $\alpha + \beta$  with the boundary surface  $Oxy$  (Fig. 1) and consisting of materials with linearly-elastic properties. We suppose that a linear source  $f_z(x, y, t)$  located anywhere on the axis  $Oy, y \leq 0$  acts, causing propagation of SH-

waves. Since the corresponding points from all planes parallel to the  $Oxy$ -plane, will oscillate in one and the same manner, it is sufficient to solve the following two-dimensional, in the plane  $Oxy$ , problem:

— Find the functions  $u_z(x, y, t)$ ,  $\tau_{xz}(x, y, t)$  and  $\tau_{yz}(x, y, t)$ , satisfying at every layer the equation

$$(1) \quad \rho_0 \frac{\partial^2 u_z}{\partial t^2} - \mu \Delta u_z = f_z, \quad \Omega \times (0, T), \quad \Omega \subset \mathbb{R}^2, \quad 0 < T < \infty,$$

and relations

$$\tau_{xz} = \mu \frac{\partial u_z}{\partial x}, \quad \tau_{yz} = \mu \frac{\partial u_z}{\partial y},$$

where  $u_z(x, y, t)$  is the displacement component on  $Oz$  axis,  $\rho_0(x, y)$  is the mass density and  $\mu(x, y)$  is the shear modulus.

In order to obtain a unique solution definite boundary conditions must be satisfied. As we solve Eq. (1) in the domain  $\Omega$  instead of the half-space  $Oxy$ ,  $y \leq 0$ , we impose in appropriate combinations the following boundary conditions:

— prescribed displacements on  $\Gamma_u \times (0, T)$

$$(2) \quad u_z(x, y, t) = U_z(x, y, t),$$

— prescribed tractions on  $\Gamma_\sigma^1 \times (0, T)$

$$(3) \quad \sigma_T = \tau_{xz} n_1 + \tau_{yz} n_2 = \mu \frac{\partial u_z}{\partial n} = F_z(x, y, t),$$

where  $n = (n_1, n_2)$  is the outward unit normal vector on  $\Gamma_\sigma^1$ ,

— of contact type (elastic contact) on  $\Gamma_\sigma^2 \times (0, T)$

$$(4) \quad \sigma_T + k u_z = 0, \quad k > 0 \text{ const.},$$

— of contact type (viscous contact) on  $\Gamma_\sigma^3 \times (0, T)$

$$(5) \quad \sigma_T + c \frac{\partial u_z}{\partial t} = 0, \quad c > 0 \text{ const.}$$

We require the following initial conditions to be satisfied

$$(6) \quad u_z(x, y, 0) = u_{z0}(x, y), \quad \frac{\partial u_z(x, y, 0)}{\partial t} = u_{z1}(x, y).$$

We suppose that  $\Omega \subset \mathbb{R}^2$  is an open, bounded domain with sufficiently smooth boundary  $\Gamma = \partial\Omega$ . Combining the boundary conditions (2)–(5) in the following way

$$(7a) \quad \Gamma = \Gamma_\sigma^1 \cup \Gamma_u, \quad \Gamma_\sigma^1 \cap \Gamma_u = \emptyset;$$

$$(7b) \quad \Gamma = \Gamma_\sigma^1 \cup \Gamma_\sigma^2, \quad \Gamma_\sigma^1 \cap \Gamma_\sigma^2 = \emptyset;$$

$$(7c) \quad \Gamma = \Gamma_\sigma^1 \cup \Gamma_\sigma^3, \quad \Gamma_\sigma^1 \cap \Gamma_\sigma^3 = \emptyset,$$

we obtain three problems, which we solve consequently.

With  $V$  and  $V_0$  we denote the following Hilbert spaces:

$$V = H^1(\Omega) = \left\{ u \mid u, \frac{\partial u}{\partial x}, \frac{\partial u}{\partial y} \in L_2(\Omega), \|u\|_1 = \|u\|_{H^1(\Omega)} \right\},$$

$$V_0 = \{ u \mid u \in V, u|_{\Gamma_u} = 0, \|u\|_{V_0} = \|u\|_1 \}.$$

We denote with  $u_z(t)$  the function  $(x, y) \rightarrow u_z(x, y, t)$  and with  $A$  — the following differential operator

$$Au_z \equiv -\mu \Delta u_z.$$

Superposed dot indicates the differentiation with respect to time. For  $\forall u, v \in V(V_0)$  with  $a(u, v)$  we denote the bilinear form

$$(8) \quad a(u, v) = \int_{\Omega} \mu \operatorname{grad} u \cdot \operatorname{grad} v d\Omega.$$

Then the following Green's formula

$$(9) \quad (Au, v) = a(u, v) - \int_{\Gamma} \mu \frac{\partial u}{\partial n} \cdot v d\Gamma,$$

is valid.

Let us formulate the problems which we solve. The weak statement of the problem (1) with boundary conditions (2)—(3) and initial conditions (6) is:

**Problem 1c.** Find the function  $t \rightarrow u_z(t): [0, T] \rightarrow V_0$ , satisfying for  $\forall v \in V_0$

$$(10) \quad (\rho_0 \ddot{u}_z(t), v) + a(u_z(t), v) = (f_z(t), v) + \int_{\Gamma_1^1} F_z(t) \cdot v d\Gamma + (\rho_0 \ddot{\Phi}(t), v) + a(\Phi(t), v)$$

and the initial conditions (6). Here  $\Phi(t)$  is a function belonging to  $V$  and satisfying the boundary conditions (2).

The weak form of the problem (1) with boundary conditions (3)—(4) and initial conditions (6) is:

**Problem 2c.** Find the function  $t \rightarrow u_z(t): [0, T] \rightarrow V$ , satisfying for  $\forall v \in V$

$$(11) \quad (\rho_0 \ddot{u}_z(t), v) + a(u_z(t), v) + k \int_{\Gamma_2^2} u_z(t) \cdot v d\Gamma = (f_z(t), v) + \int_{\Gamma_1^1} F_z(t) \cdot v d\Gamma$$

and the initial conditions (6).

The problem (1) with boundary conditions (3), (5) and initial conditions (6) has the following weak form:

**Problem 3c.** Find the function  $t \rightarrow u_z(t): [0, T] \rightarrow V$ , satisfying for  $\forall v \in V$

$$(12) \quad (\rho_0 \ddot{u}_z(t), v) + a(u_z(t), v) + c \int_{\Gamma_3^3} \dot{u}_z(t) \cdot v d\Gamma = (f_z(t), v) + \int_{\Gamma_1^1} F_z(t) \cdot v d\Gamma$$

and the initial conditions (6).

### 3. Finite element approximation

Discretizing  $\Omega$  by linear or quadratic triangular and bilinear or biquadratic quadrilateral finite elements, we obtain the following discrete problems corresponding to the problems 1—3.

**Problem 1d.** Find the function  $t \rightarrow r(t): [0, T] \rightarrow R^G$  ( $G$  — number of nodes in the finite element mesh) satisfying for  $\forall t \in [0, T]$  the system of equations

$$(13) \quad Mr''(t) + Kr(t) = R(t)$$

and the initial conditions

(14)

$$r(0) = p_0, \quad \dot{r}(0) = p_1.$$

**Problem 2d.** Find the function  $t \rightarrow r(t): [0, T] \rightarrow \mathbb{R}^G$ , satisfying for  $\forall t \in [0, T]$  the system of equations

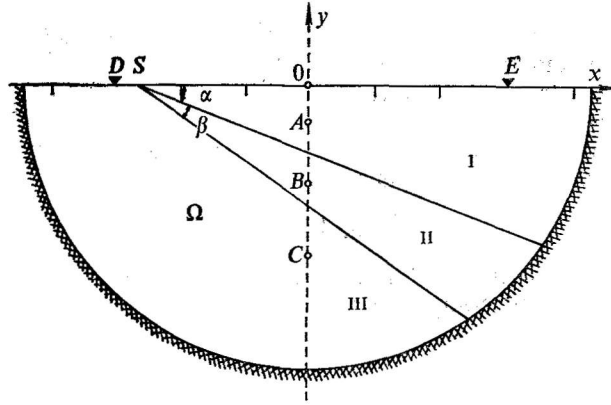


Fig. 1. Half-space with dipping layers

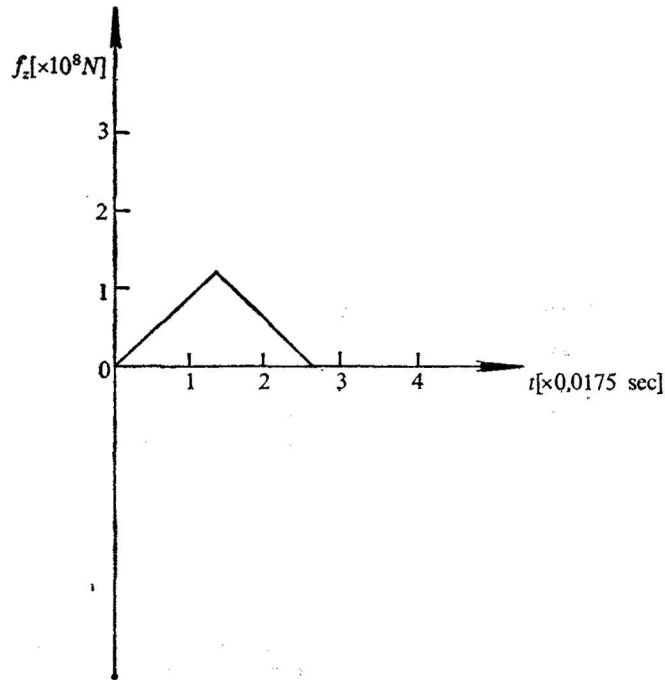


Fig. 2. Diagram of the  $z$ -component of the source

(15)

$$M\ddot{r}(t) + K_r r(t) + Kr(t) = R(t)$$

and the initial conditions (14).

**Problem 3d.** Find the function  $t \rightarrow r(t): [0, T] \rightarrow \mathbb{R}^G$ , satisfying for  $\forall t \in [0, T]$  the system of equations

$$(16) \quad M\ddot{r}(t) + C_i\dot{r}(t) + Kr(t) = R(t)$$

and the initial conditions (14).

In the expressions (13)—(16) the following notations are used: with  $M$  and  $K$  the mass and stiffness matrices are denoted;  $K_i$  and  $C_i$  are the matrices obtained when the boundary conditions (4) and (5) are applied on  $\Gamma_\sigma^2$  and  $\Gamma_\sigma^3$ , respectively;  $r(t)$  and  $R(t)$  are vectors with components the values of the displacement and load in the nodes of the mesh;  $p_0$  and  $p_1$  are a priori known vectors with components the values of the displacement and velocity at  $t=0$ .

The energy dissipation could be taken into account as complex shear modulus for the material of every finite element  $e$  is used

$$(17) \quad \mu_e^* = \mu_e(1 + i\beta_e),$$

where  $\beta_e$  is the damping coefficient for this material. In this case the components of the stiffness matrix  $K$  will be complex numbers.

#### 4. Numerical results

The domain  $\Omega$  having the form of a semicircle with radius 150 m is considered. Angles  $\alpha=20^\circ$  and  $\beta=15^\circ$  and characteristics for the soil layers are chosen as follows:

Ist layer —  $\mu_1=0.1 \times 10^{12}$  Pa,  $\rho_0=2500$  kg/m<sup>3</sup>,

IInd layer —  $\mu_2=0.2 \times 10^{12}$  Pa,  $\rho_0=2500$  kg/m<sup>3</sup>,

IIIrd layer —  $\mu_3=0.4 \times 10^{12}$  Pa,  $\rho_0=2500$  kg/m<sup>3</sup>.

Due to the excitation shown in Fig. 2 the displacement and stress fields are obtained. Figs 3—11 contain displacement diagrams of the points  $E(105$  m,  $0$ m),  $D(-105$  m,

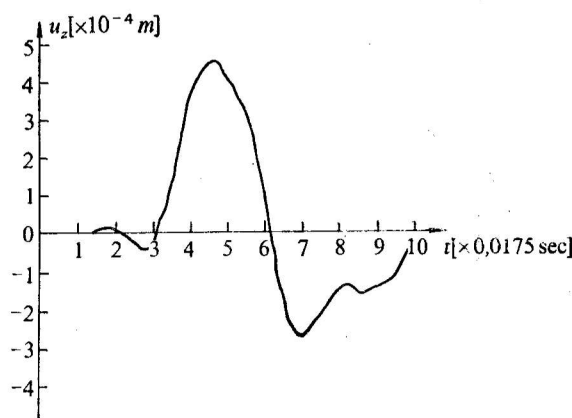


Fig. 3. Displacement diagram for the point  $D(E)$ , obtained when problem 1 is solved for one-layered media with excitation located in the point  $A$

$0$ m), as the excitation  $f_2(x, y, t)$  is located in some of the points  $O(0$ m,  $0$ m),  $A(0$ m,  $-17.5$  m),  $B(0$ m,  $-52.5$  m) or  $C(0$ m,  $-87.5$  m) and  $SO=90$  m.

Firstly, the case  $\alpha=180^\circ$ ,  $\beta=0^\circ$ , i. e. the media with the properties of the Ist layer, is considered. In Figs 3—4 the displacement diagrams of the point  $D(E)$  are given, obtained when the problem 1d with excitation located at the point  $A$  is solved. The

results from Fig. 4 are obtained for the case when the dissipation of the energy is taken into account (the damping coefficients are taken one and the same for all of the finite elements  $-\beta_e=0.1$ ). In Figs 5–6 the diagrams of the displacement in the point  $D(E)$  are given, obtained when problems 2d-3d are solved, as the excitation is

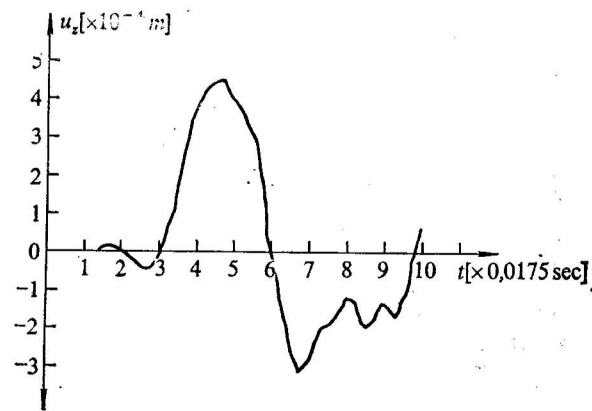


Fig. 4. Displacement diagram for the point  $D(E)$ , obtained when problem 1 is solved for one-layered media with excitation located in the point  $A$  and when damping is taken into account with coefficients  $\beta_e=0.1$  for  $\nabla e$

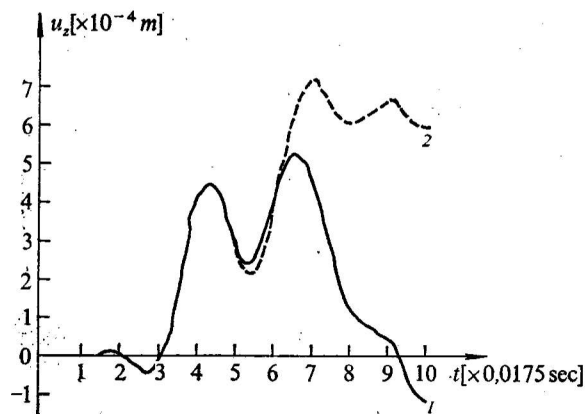


Fig. 5. Displacement diagrams for the point  $D(E)$ , obtained when problem 2 is solved for one-layered media with excitation located in the point  $A$  and with coefficients  $k=10^8$  Pa/m — curve 1,  $k=10^4$  Pa/m — curve 2

located in the point  $A$ . The following values of the constants  $k$  and  $c$  are used:  $k=10^8(10^4)$  Pa/m,  $c=10^8(10^4)$  Pa . sec/m.

Fig. 7 contains the displacement diagrams obtained for points  $D$  and  $E$  when the problem 1d is solved for two-layered media ( $\alpha=20^\circ$ ,  $\beta=160^\circ$ ), as the excitation is located in the point  $A$ .

In Figs 8–11 the diagrams of the displacements for the points  $D$  and  $E$ , obtained when the problem 1d for three-layered media ( $\alpha=20^\circ$ ,  $\beta=15^\circ$ ) is solved. In this case the excitation is located in the points  $O$ ,  $A$ ,  $B$  and  $C$ , consequently.

All results presented are obtained using Wilson's  $\theta$ -method ( $\theta=1.4$ ) with time step  $\Delta t=0.00175$  sec. The problems are also solved by means of Fast Fourier Transform. About two times less computational work is done in this case, but a good results are obtained only when the dissipation of the energy is accounted. This could

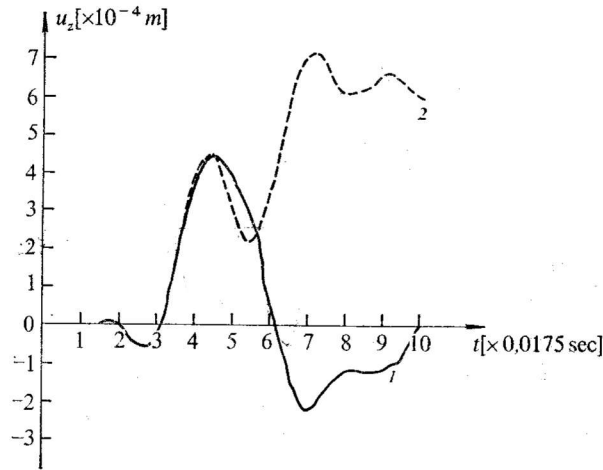


Fig. 6. Displacement diagrams for the point  $D(E)$ , obtained when problem 3 is solved for one-layered media with excitation located in the point  $A$  and with coefficients  $c=10^8$   $Pa/m$ . sec — curve 1,  $c=10^4$   $Pa/m$ . sec — curve 2

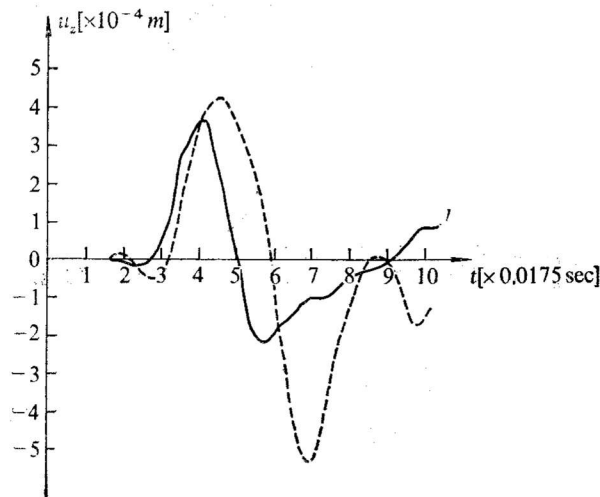


Fig. 7. Displacement diagrams in the points  $D$  — curve 1 and  $E$  — curve 2, obtained when problem 1 is solved for two-layered media with excitation located in the point  $A$

be explained with the fact that loading frequency spectrum covers the frequency spectrum of the domain under consideration, when the time step  $\Delta t$  is very small. Increasing of  $\Delta t$  leads to a bad description of the loading, as well as of the displacement and stress fields.

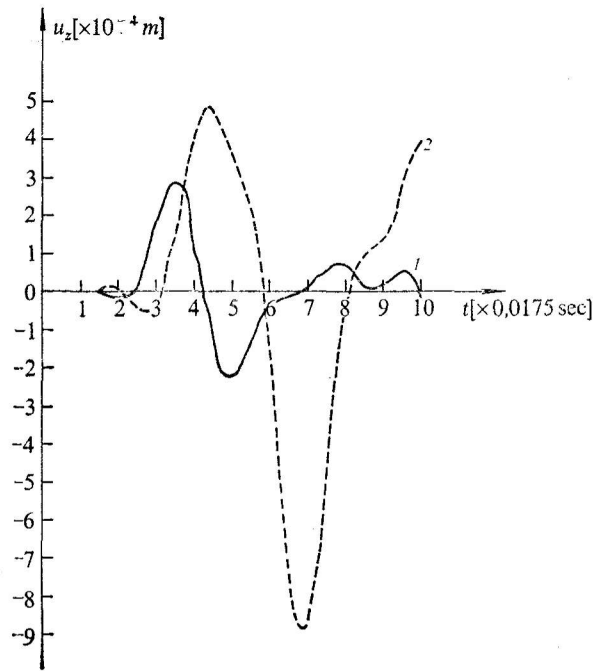


Fig. 8. Displacement diagrams in the points  $D$ —curve 1 and  $E$ —curve 2, obtained when problem 1 is solved for three-layered media with excitation located in the point  $O$

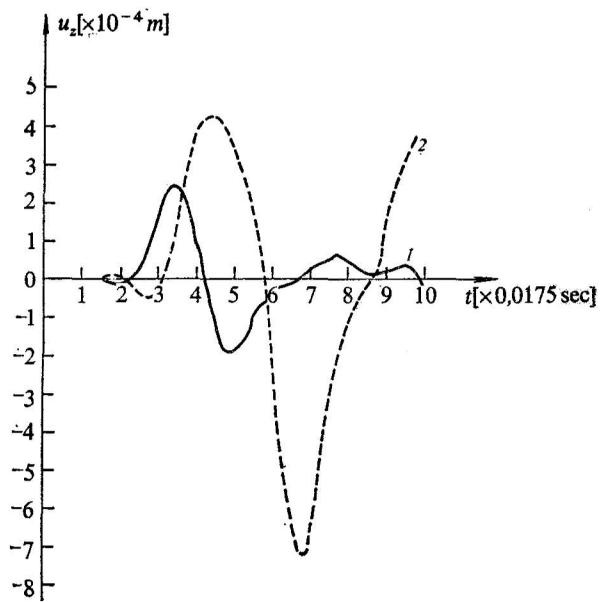


Fig. 9. Displacement diagrams in the points  $D$ —curve 1 and  $E$ —curve 2, obtained when problem 1 is solved for three-layered media with excitation located in the point  $A$

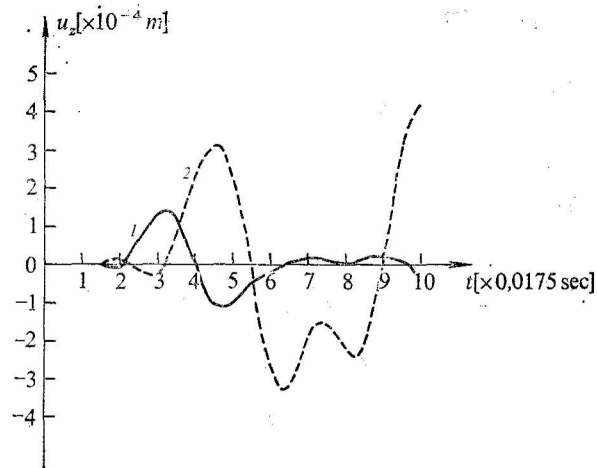


Fig. 10. Displacement diagrams in the points  $D$ —curve 1,  $E$ —curve 2, obtained when problem 1 is solved for three-layered media with excitation located in the point  $B$

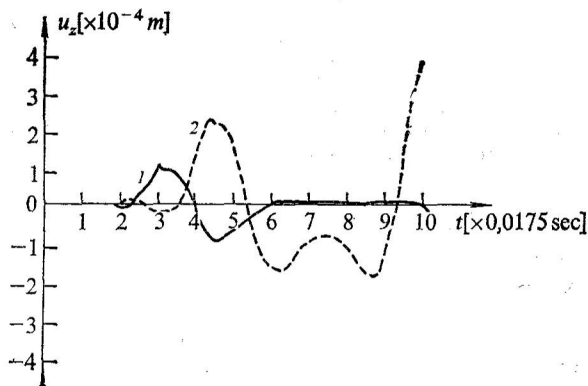


Fig. 11. Displacement diagrams in the point  $D$ —curve 1,  $E$ —curve 2, obtained when problem 1 is solved for three-layered media with excitation located in the point  $C$

## 5. Conclusion

In this paper different types of boundary conditions which compensate the restriction of the half-space in a finite domain are considered. Displacements diagrams for points of the surface are obtained. They could be used for comparison with results obtained by other methods — numerical or experimental. Here we shall outline some peculiarities of the problems 1—3. It is advisable to solve problem 1 when we knew the values of the displacements on  $\Gamma_w$ . In most cases, however, these values are not known a priori. Then we could obtain reasonable results imposing homogeneous boundary conditions on  $\Gamma_w$ , when sufficiently large domain is considered, since the waves are damped with the distance from the source point. It is appropriate to solve problems 2—3 when contact characteristics  $k$  and  $c$  for  $\Gamma_\sigma^2$ ,  $\Gamma_\sigma^3$  are known. Identical results are obtained when we solve the problems 2—3 with large

values of the constants  $k$  and  $c'$  (greater than  $10^{12}$ ) and problem I with homogeneous boundary conditions on  $\Gamma_u$ .

All results in this work are obtained with the help of the computer code "SH".

## References

1. Grinchenko, V. T., V. V. Meleshko. *Garmonicheskie kolebania i volni v uprugih telah*. Kiev, "Naukova dumka", 1981.
2. Lysmer, J., G. Waas. Shear waves in plane infinite structures. — J. Eng. Mech. Div., Vol. 96, EM1, 85-104, 1972.
3. Chen, J. -C., J. Lysmer, H. B. Seed. Analysis of local variations in free-field ground motion. Berkeley, Cal., EERC 1981/03.
4. Wolf, J. P. Dynamic soil-structure interaction. Prentice-Hall Inc., Englewood Cliffs., N. Y., 1985.
5. Pao, Y. -H., C. C. Mow. Diffraction of elastic waves and dynamic stress concentrations. Crane Russak, N. Y., 1973.
6. Pao, Y. -H., R. R. Gajewsky. The generalized ray theory and transient responses of layered elastic solids. — (W. P. Mason and R. N. Thurson eds.) Physical acoustics, Vol. 13, 184-265. Academic Press, N. Y., 1977.
7. Pao, Y. -H., F. Ziegler, P. L. Chen. Analysis of transient waves in layered media with dipping structures. — In: Proceedings of the Eight World Conference on Earthquake Engineering, Vol. 2, July 21-28, 1984, San Francisco, California.
8. Pao, Y. -H., F. Ziegler. Transient SH-waves in wedge-shaped layers. — Geoph. J. R. Astr. Soc., Vol. 71, 57-77, 1982, 9.
9. Ziegler, F., Y. -H. Pao. Theory of generalized rays for SH-waves in dipping layers. — Wave motion, Vol. 7, 1-24, 1985, North-Holland, Amsterdam.
10. Ziegler, F., Y. -H. Pao, Y. S. Wang. Transient SH-waves in dipping layers, the buried line-source problem. — J. Geoph., Vol. 57, 23-32, 1985.
11. Ziegler, F., Y. -H. Pao, Y. S. Wang. Generalized ray-integral representation of transient SH-waves in a multiply layered half-space with dipping structure. — Acta Mechanica, Vol. 56, 1-15, 1985.
12. Lysmer, J., R. L. Kuhlemeyer. Finite dynamic model for infinite media. — J. Eng. Mech. Div., Vol. 95, EM4, 859-877, 1969.
13. Zienkiewicz, O. C., K. Morgan. Finite elements and approximations. John Wiley & Sons Inc., N. Y., 1983.
14. Brebbia, C. A., S. Walker. Boundary element technics in engineering. Newness-Butherworths, 1980.
15. Angelov, T. A., Ts. P. Ivanov. On a model for determining the response of underground structures to earthquake motions. Third conference on differential equations and applications, Russe, Bulgaria, 1985.

*Received 28. 07. 1987*